Dynamic Response Analysis of Quasi Z-source Based Fuel Cell with Super Capacitor

Mehdi Alemi Rostami*
Corresponding Author
Department of Research center of Aeronautical Science and Technology
Research Institute of Aerospace,Iran

Abstract
In this paper, the dynamic analysis of the quasi z-source inverter control system is considered as the interface converter for fuel cell. For this purpose, the dynamic modeling of the fuel cell and its interface converter are used to design controllers. However, due to the slow dynamics of the fuel cell, its high equivalent impedance, the existence of zero right in the dynamical model of the z-source inverter, as well as the dependence of the z-source inverter modulation system on the dynamic response, the fuel cell system stability limit and its interface converter is low. In order to improve the dynamic performance of the fuel cell system, this paper uses a super capacitor in parallel with a fuel cell. By dynamic modeling of the fuel cell system and its interface converter, it can be concluded that the use of super capacitor closes the dynamic model of the fuel cell into an ideal voltage source and improves the stability of the z-source inverter control system. In this case, when the fuel cell system cannot be controlled alone, adding super capacitor will result in quite stable performance of system. The system performance introduced by simulation is used in MATLAB / Simulink environment.

Key words:
Dynamic Analysis, quasi z-source inverter, interface converter, fuel cell

1. Introduction

Reducing fossil fuel reserves, environmental issues, and technology growth in the production of new energy systems led to increase the use of scarce resources in low powers. Currently, Fuel Cell is considered as one of the most considerable sources of new energy, which is capable of generating a controlled power, and supply the power required for its local loads even in the absence of the main network. High efficiency, stable performance, no noise generation, non-use of moving parts and the need for minor repairs are one of the main benefits introduced by fuel cell [1].
However, due to the low response speed and the inability to generate oscillating power, energy storage systems such as batteries and super capacitor are used alongside fuel cells. In reference [2], a super capacitor alongside a fuel cell has been used to improve dynamic performance. In a fuel cell system, electronic converters of interface power are used to convert the voltages and DCs of the source to the AC voltage with 50Hz and 60Hz, and to increase the voltage level of the fuel cell to the AC side voltage level. In reference [3], the design of the fuel cell interface converter control system has been investigated. In reference [4], the design of a converter for combining a fuel cell with an energy storage source has been investigated. In reference [5], a dynamic fuel cell model with dynamic of interface converter is used to verify the stability of a dc / dc converter connected to a fuel cell. In this reference, it has been shown that the equivalent impedance of the tonen seen from the fuel cell has a negative effect on the stability of the interface converter [6].
Pulse width modulation-based inverters are used in many applications such as connecting renewable energy sources such as photovoltaic system and wind turbines to the network, fuel cell control, control AC machines, distributed generation sources, etc to convert DC to AC voltages. At present, the voltage source inverter (VSI) is the most common inverter used to convert DC to AC voltage and vice versa. However, this inverter is only one reducing inverter from DC to AC, and cannot be used in applications where a higher voltage level is required on the AC side. This type of inverter is also sensitive to noise and electromagnetic interactions (EMI), in which the unintentional and simultaneous ignition of both high and low switches of the inverter phases leads to the disappearance of the switches.
The Z-Source inverter, introduced in [7], is an inverter of an increasing-decreasing class. In this type of inverter, no additional DC / DC converter has been used to increase the DC source voltage level, and the voltage enhancement capability is obtained by inserting an impedance network between the DC source and the inverter. In this structure, by assigning short circuits for the legs of the inverter in the modulation algorithm, DC source voltage increases. As stated above, an increase in the voltage level in this type of inverter is done using the shortening of the legs of the inverter that in the inverter, the source of the voltage, was not permitted so this type of inverter is not sensitive to electromagnetic interferences.
Due to the advantages of using the z-source inverter, this type of inverter is used in many applications, such as a

Manuscript received January 5, 2018
Manuscript revised January 20, 2018

fuel cell that requires converting voltages and DC to AC voltages. In reference [8], a Z-source inverter is used as an interface converter for a PV system. In references [9] and [10], a robust PEI system with high reliability for a wind turbine based on the Z-source inverter has been introduced. In reference [11], the Z-source inverter is also used to control uninterruptible power supply. In reference [12], to improve the power quality of a network, a Z-source inverter is used to reduce voltage harmonics. In references [15] - [13], the Z-source inverter is used as a converter to control the fuel cell.

Due to the structure of a Z-source inverter to increase the voltage level and convert the inverter voltage, the modulator coefficient and inverter shortening ratio depend on each other and limit each other in a high amount. In order to reduce the stress of the voltage on the inverter switches, always tried to convert the voltage with the highest modulation coefficient and the lowest shortening coefficient, in this way the maximum boost control (MBC) and the maximum constant boost control (MCBC) in [16] and [17] is introduced. In addition to switching control methods to reduce voltage stress on the switches, more advanced structures of the Z-source inverter with higher voltage gain are introduced. In [18], the structure of the inverter switched inductor is introduced, which uses 6 diodes in the impedance network to increase the voltage gain. In [19], the structures of Trans Z-source inverters have been introduced in which a high-frequency transformer on the impedance network is used. [20] Extended boost structures have been introduced that is use a greater number of elements on the DC side to increase the voltage gain. An asymmetric Γ-Source inverter that is introduced in reference [21] is a high-voltage inverter with a high frequency transformer based in the impedance network. In this type of structure, a high-voltage gain is obtained with a lower-than-low ratio compared to other transformer-based structures. Reducing the transverse ratio reduces transducer volume and reduces the stress on the inverter switch.

To control the Z-source inverters, a dynamic model of this type of inverter is used. In the references [22] and [23], the Medium Matrix Method is used for dynamical modeling of the impedance network. In [24], a two-ring control system is designed based on the model derived from the system. In [25], a Quasi Z-source inverter was modeled and controlled for use in distributed generation systems. Despite the advantages of using the z-source inverter, the stability of this type of inverter is low due to the right zero in the dynamical model of the impedance network. However, due to the simple structure, the continuous flow absorption of the source and the reduction of the rating of the devices used in the impedance network, the quasi-z-source inverter is the most popular type of z-source family inverter.

In this paper, the quasi z-source inverter is used to drive a fuel cell in the mode of independent performance. In order to verify the dynamics of the system, the modeling of interfacial converter state and fuel cell is used. In order to improve the dynamic performance of the control system and increase the stability of the quasi z-source inverter control system with zero of right side, a super capacitor in the impedance network is used. Dynamic analyzes show that the use of this super capacitor results in increasing control, stability and improving performance of the inverter modulation system during transient states. In order to verify the performance of the system introduced, MATLAB/ simulink software simulations are used.

2. Dynamic fuel cell model connected to the quasi z-source inverter

The structure of the system introduced in Figure 1 is shown. In this structure, an impedance network is used to increase the voltage level. In this structure, it can be used a super capacitor in parallel with the fuel cell as shown in Fig. 1. In order to check the performance of this type of inverter, the equivalent circuit of this type of inverter is used in both the shortening and non-short-circuit connections shown in Figures 2a and 2b, respectively. In this figure, the flow rate is modeled by the current source (io) and the S switch is used to model the switching function of the inverter. When connected, the S switch is turned on and the inverter output is short-circuited. In this case, the energy stored in the capacitors and the source is stored in the inductors. In this case, the diode D is in reverse bias state. In non-short-circuit mode, the switch S is turned off and the load current is supplied from the impedance network. In this case, the energy stored in the inductors is evacuated in the capacitors and leads to an increase in the voltage level of the DC source. In this case, the diode D in the impedance network is in direct bias state.

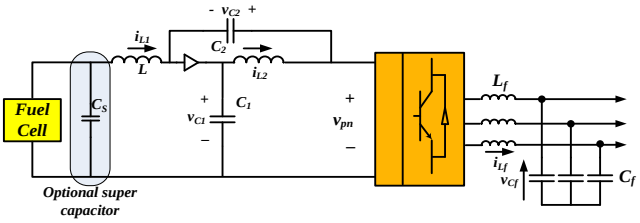

Fig. 1 The structure of the system introduced

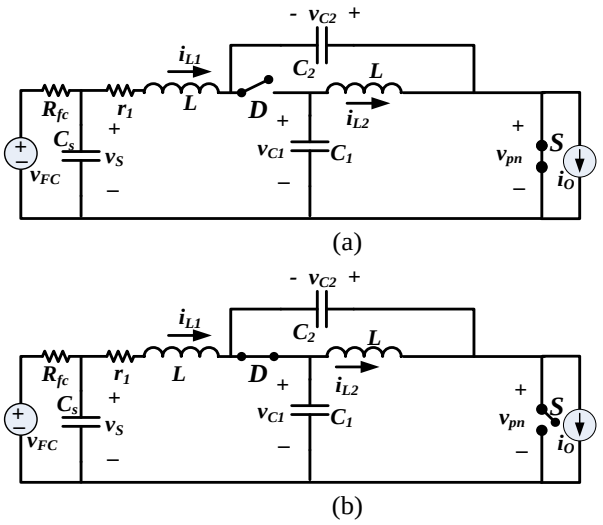

Fig. 2 Inverter model, (a) in short circuit mode, (b) in non-short circuit mode.

In order to model the performance of the fuel cell, the electric fuel cell model shown in Fig. 3 is used [2]. In this figure, Zfc represents the fuel cell tonen impedance. Due to the fact that the fuel cell dynamics is much slower than the interfacial converter dynamics, it can be ignored the dynamics of the fuel cell in transient states compared to the interface converter. Therefore, without loss of generality of the problem, it can be assumed fuel cell as a voltage source without a dynamic series with a resistance. According to Fig. 3, the equivalent impedance of a fuel cell is obtained by the relation (1).

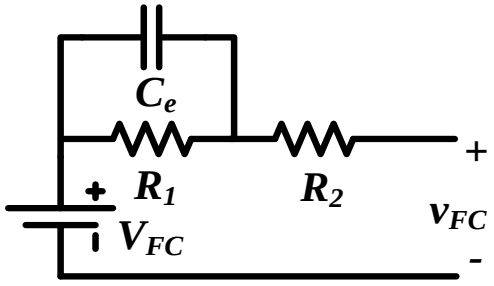

Fig. 3 Fuel Cell Dynamic Model

$$Z_{fc}(s)=\frac{R_1R_2C_1s+R_1+R_2}{R_1C_1s+1} \quad (1)$$

In Fig. 4, a Bode diagram of fuel cell tonen for a system with R1 = 0.1Ω, R2 = 0.5Ω and C1 = 0.1F is shown. As can be seen, at high frequencies, the performance of a fuel cell is similar to an ideal voltage source with a resistor that has the same response to all frequencies.

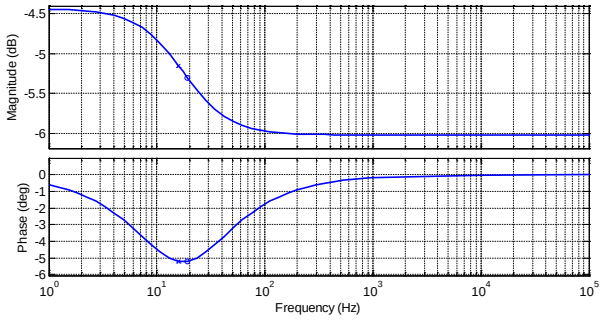

Fig. 4 Bode diagram of fuel cell tonen impedance

According to Figure 4, in transient conditions, due to the higher bandwidth of the interface converter compared to the fuel cell, the impedance Zfc is as a series resistance with the ideal voltage source Vfc.. In this case we have

$$Zfc=Rfc \quad (2)$$

In Fig. 5, the current voltage characteristic for a fuel cell is displayed. As can be seen, the fuel cell function is divided into three regions: activation of polarization, ohmic polarization, and concentration polarization. Naturally, the fuel cell works in the area of ohmic polarization, which is stable and high performance area. For a fuel cell with the voltage-current specification shown in Figure 5, the Rfc is about 0.3-0.6Ω. Nevertheless, in real applications, in order to increase the final voltage level of the system, parallel and series combinations of fuel cell are used. In this case, the fuel cell's equivalent resistance may be several times of the value shown in Figure 5.

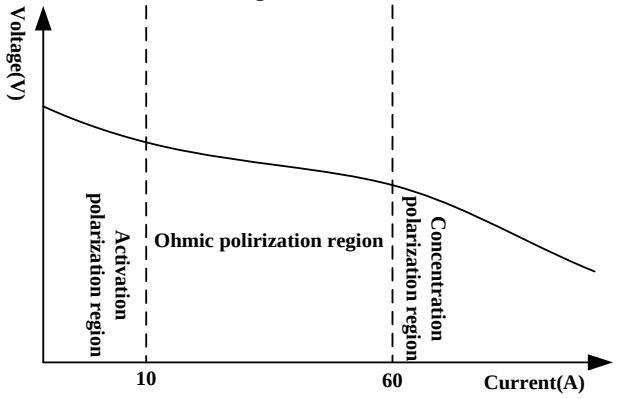

Fig. 5 polarization curve of fuel cell

After introducing the dynamic model of fuel cell, this section focuses on the quasi-z-source inverter modeling. To obtain the dynamical model of the impedance network, equations of state of the system in Figures 2a and 2b are used. In the short-circuit condition, the system state equations are as follows.

$$\frac{dx}{dt} = A_{st}\,x + B_{st}\,u_0 \tag{2}$$

Where

$$x = \begin{bmatrix} i_{L1} & i_{L2} & v_{C1} & v_{C2} & v_S \end{bmatrix}^T \quad u_0 = \begin{bmatrix} i_O \\ v_{FC} \end{bmatrix}$$

$$A_{st} = \begin{bmatrix} -r/L & 0 & 0 & 1/L & 1/L \\ 0 & -r/L & 1/L & 0 & 0 \\ 0 & -1/C & 0 & 0 & 0 \\ -1/C & 0 & 0 & 0 & 0 \\ -1/C_S & 0 & 0 & 0 & -1/R_{fc}C_S \end{bmatrix}, \quad B_{st} = \begin{bmatrix} 0 & 0 \\ 0 & 0 \\ 0 & 0 \\ 0 & 0 \\ 0 & 1/R_{fc}C_S \end{bmatrix} \tag{3}$$

In non-short-circuit mode, the equations of state in Fig. 2b are written as follows

$$\frac{dx}{dt} = A_{nst}\,x + B_{nst}\,u_0 \tag{4}$$

$$A_{nst} = \begin{bmatrix} -r/L & 0 & -1/L & 0 & 1/L \\ 0 & -r/L & 0 & -1/L & 0 \\ 1/C & 0 & 0 & 0 & 0 \\ 0 & 1/C & 0 & 0 & 0 \\ -1/C_S & 0 & 0 & 0 & -1/R_{fc}C_S \end{bmatrix}, \quad B_{nst} = \begin{bmatrix} 0 & 0 \\ 0 & 0 \\ -1/C & 0 \\ -1/C & 0 \\ 0 & R_{fc}C_S \end{bmatrix} \tag{5}$$

The equations of average mode of the impedance network are written as follows.

$$\frac{dx}{dt} = Ax + B\,u_0, \qquad y = C_0 x \tag{6}$$

Where

$$A = D.A_{st} + (1-D).A_{nst}$$

$$= \begin{bmatrix} -r/L & 0 & (D-1)/L & D/L & 1/L \\ 0 & -r/L & D/L & (D-1)/L & 0 \\ (1-D)/C & -D/C & 0 & 0 & 0 \\ -D/C & (1-D)/C & 0 & 0 & 0 \\ -1/C_S & 0 & 0 & 0 & -1/(R_{fc}C_S) \end{bmatrix}$$

$$B = D.B_{st} + (1-D).B_{nst} = \begin{bmatrix} 0 & 0 \\ 0 & 0 \\ (D-1)/C & 0 \\ (D-1)/C & 0 \\ 0 & 1/R_{fc}C_S \end{bmatrix},$$

$$C_0 = \begin{bmatrix} 1 & 0 & 0 & 0 & 0 \\ 0 & 0 & 1 & 0 & 0 \end{bmatrix} \tag{7}$$

Considering the small signal changes of equation (13) around a certain point, the changes D around the point of work $\hat{d}$ also appear as an input, leading to a change in the structure of the matrix B and u as follows. Given that in the design studies of the control system, the unloaded fuel cell voltage does not appear as a disturbance, here, without loss of generality, the problem is assumed vFC = 0

$$u = \begin{bmatrix} \hat{D} & \hat{i}_o \end{bmatrix}^T$$

$$B = \begin{bmatrix} (V_{C1}+V_{C2})/L & 0 \\ (V_{C1}+V_{C2})/L & 0 \\ (Io-I_{L1}-I_{L2})/C & (D-1)/C \\ (Io-I_{L1}-I_{L2})/C & (D-1)/C \\ 0 & 0 \end{bmatrix} \tag{8}$$

Where IL1, IL2, Io, VC1 and VC2 respectively L1 inductance currents, L2 inductance, output current, C1 and C2 capacitor voltage are specified at a point of operation. According to equations (6) and (8), the system descriptor equation in the Laplace domain is obtained as follows

$$G_{\hat{D}}^{\hat{v}_{C1}} = \frac{\hat{v}_{C1}}{\hat{D}} = \begin{bmatrix} 0 & 0 & 1 & 0 & 0 \end{bmatrix}.(sI - A)^{-1} B \begin{bmatrix} 1 & 0 \end{bmatrix}^T \tag{9}$$

This conversion function is used to design the interface inventer control system. Indeed, (9) it is the function of system closed loop conversion that correlates the changes in the shoot through duty cycle to the capacitor voltage. In the fuel cell control system, this conversion function is used to control the voltage of the C1 capacitor to increase the DC input voltage level of the DC source.

3. Analysis of fuel cell control system and quasi z-source inverter

The structure of the control system presented in Figure 6 is shown. In order to increase the voltage level of the fuel cell to an appropriate voltage level for controlling the AC voltage side, a linkage of control of capactor voltage of the middle link of the impedance network is used. In a z-source family of inverter, the reference voltage range of the C1 capacitor is governed by equation (10) for the simple boost control method.

$$V_{C1} \geq 2V_{in} \tag{10}$$

If the inequality condition (10) is established, in the quasi z-source inverter modulation, the active vector intervals are not degraded by the shoot-through intervals and the operation of the control system of the impedance network does not interfere with the AC-side function. In order to control the AC voltage side, this paper uses a two-loop

control system consisting of an internal flow controller and an external voltage controller. In order to achieve high bandwidth, high stability limit and zero-mode fault in voltage control, PI control systems in the synchronous reference frame are used. The system parameters on the AC side are listed in Table 1.

Table 1: Specifications of the system on the AC side

Parameters	Values
Current control loop PI (kp, ki)	(10.5, 16000)
Current control loop PI (kp, ki)	(0.1, 300)
Capacitor Filter (Cf)	45µF
Inductor Filter (Lf)	1.8mH
Inductor resistance (rLf)	0.1 Ω
Nominal Frequency	50 Hz
Nominal Voltage	120 V (RMS) phase-null

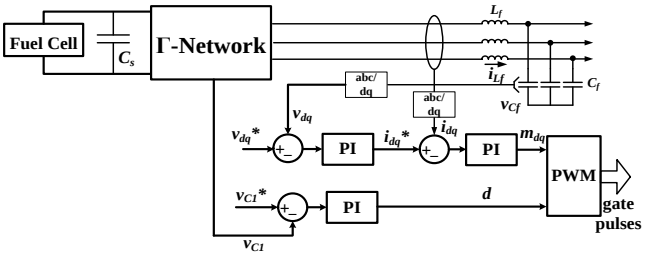

Fig. 6 Fuel cell control system structure

In order to control the voltage of the capacitor side of the impedance network, it is necessary to use the dynamic model of the converter and fuel cell. The Bode diagram of the GVC2-d conversion function for different values of Rfc is shown in Fig. 7. If Rfc = 0, in this case the fuel cell source appears as an ideal voltage source. In addition, as shown in Fig. 7, by changing the equivalent value of the fuel cell's equivalent, the Bode diagram displayed for voltage control changes. In this case, the Rfc value affects the dynamics of the system. In the drawing of the Bode diagram of figure 7, the parameters listed in Table 2 are used. According to Figure 7, in the cases of high-resistance fuel cell, the frequency response of the system decreases, indicating a decrease in system bandwidth and system response speed.

Table 2: arameters of the studied system

Parameters	Values
Impedance network Capacitors (C)	400uF
Impedance network inductors (L)	0.5mH
Inductor parasitic resistance (r)	0.1ohm
D	0.3
Io, IL1, IL2	23, 35, 35
Vc1, Vc2	700, 250
VFC (Nominal)	450V

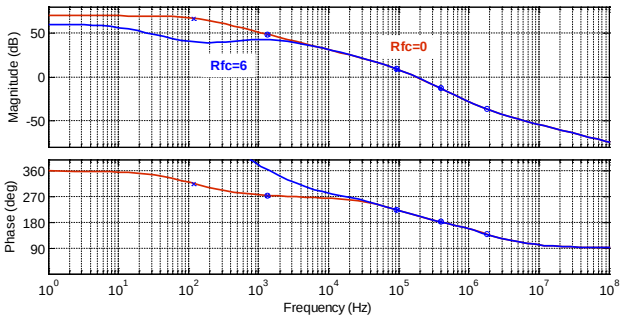

Fig.6 The Bode Diagram of the GVc1-d conversion function

In Figure 7, the Bode diagram of a system controlling the C1 capacitor voltage for various RFC modes. As seen in these figures, by increasing RFC value, the bandwidth of the control system decreases. In fact, by reducing the bandwidth of the control system, the vC1 voltage recovery rate is reduced to the reference value by the control system. This reduction in the voltage recovery in the impedance source inverters leads to an increase in the interference range of the active switching vectors and shortening vectors. If this problem persists, there is the possibility of a z-source inverter that fully enters the range of instability. In Fig. 8, the kp and ki values of the control system are assumed 0.0002 and 0.1, respectively. These values are desirable for controlling an ideal source voltage system. Nevertheless, due to fuel cell constraints, the response of these coefficients for a quasi-z-source inverter system connected to a fuel cell is weak.

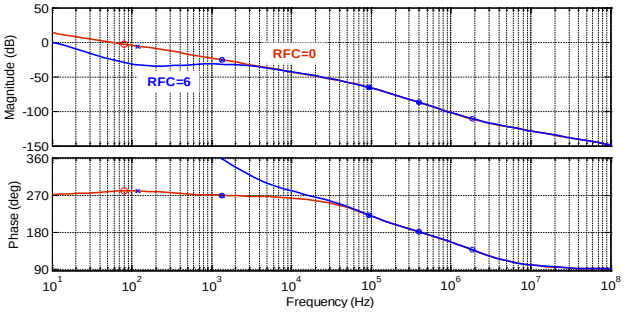

Fig.7 Bode diagram of designed control system for Rfc different mode

As shown in Figures 6 and 7, the effect of the equivalent fuel cell resistance on the control system appears as a negative effect on the control system. In fact, during the transient moments of the inverter, sudden charge changes lead to a dramatic change in the output voltage of the fuel cell with a high equivalent resistance, which adversely affects the control system. However, if it can be created conditions using energy storage systems such as super capacitor that the performance of the fuel cell to be closed to an ideal voltage source at low frequencies, thereby there is the possibility of increasing the stability of the system.

In this part, the comparison of the presence and absence of a capacitor for a fuel cell with a resistance of 0.6ohm is used to clarify the effect of using a fuel cell.
In Figure 8, the bode diagram of a control system with PI controller coefficients cited is drawn for two states of Cs = 100uF and Cs = 0.5F. In Figure 8 it is clear that the existence of parallel super capacitor with the fuel cell led to improve system bandwidth. In this case, in the event of a turbulence caused by the load, the high voltage drop occurred at the outlet of the fuel cell does not result in instability problems or modulation performance impairment. As shown in Figures 7 and 8, the use of a super-capacitor provides not only an energy buffer for super capacitor, it can provide oscillatory power for unbalanced loads, it can increase system stability, and provides the design of the system of higher bandwidth control.
As stated above, the purpose of the super capacitor is to compensate the frequency characteristic of the fuel cell. In order to investigate the use of super capacitor to improve the characteristic of the fuel cell impedance, bode diagram 9 is used. As can be seen, the system Bode diagram with capacitor heads 5F and a resistivity equivalent to Rfc = 6ohm is very close to a system Bode diagram with a low resistivity without super capacitor. From the comparison of Fig. 9, it can be concluded that the use of super capacitor causes the closeness of performance of source of the fuel cell to the ideal voltage source. In fact, in order to eliminate the undesirable effect of the presence of Rfc, the super capacitor of Cfc is used.

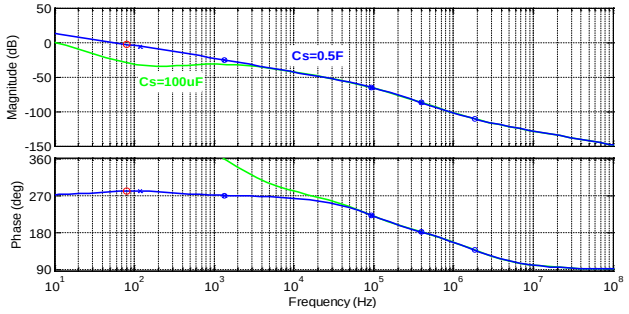

Fig. 8 Bad drawn diagram for different input capacitor states

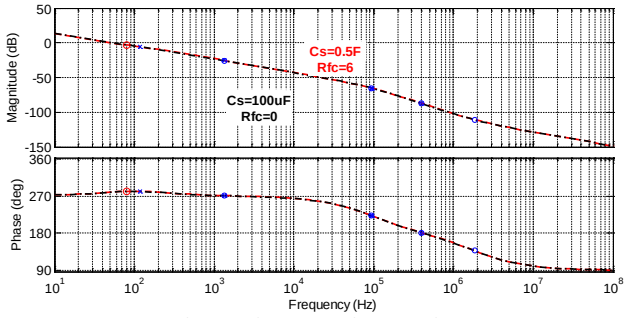

Fig. 9 Comparison of the performance of parallel fuel cell with supper capacitor with ideal voltage source

4. Simulation and evaluation

In this section, for simulation of system's performance designed, the stimulations of MATLAB / simulink software are used. To this end, the system's performance is evaluated in three ways. In the first case, it is assumed that the system initially was feeding a load 14kW and suddenly the system load from an initial value increases to 28kW. Initially, the performance of a system with ideal voltage source as a DC source is investigated. After analyzing the system's response to load disturbances, the next step is to simulate a real fuel cell with a resistance of 6ohm and an output voltage of 660V which produces a current of 35A. In this section, a typical filter capacitor is used in parallel with a fuel cell. In the final stage, the effect of using super capacitor on the performance of the fuel cell is studied.
In simulations of this section, at t = 0.2s, the charge on the AC side suddenly doubles. In this section assumed that the DC source is an ideal source of 450V, with a series with a small resister 0.06ohm and is as parallel with a capacitor Cs = 100uF. The load current is shown in Figure 10a, which is increased with increasing load. In Figure 10b, the load voltage is displayed. Due to the AC-side system's supply to high-bandwidth controllers, increasing the load not led to a voltage control error. In Fig. 10c, the capacitor voltage C1 is shown. Considering that the capacitor voltage C1 returns to the initial value immediately after deviating from its reference value, It can be concluded that the control system designed for an ideal voltage source on the DC side has no problem. In Figure 11 a, the signals of inverter's modulation are depicted. As can be seen, in this figure, there is no interference between the sine reference signals and the direct-generation signals of short-circuit arrays. In Fig. 11b, the flow drawn from the fuel cell is shown, which begins to increase with increasing load.

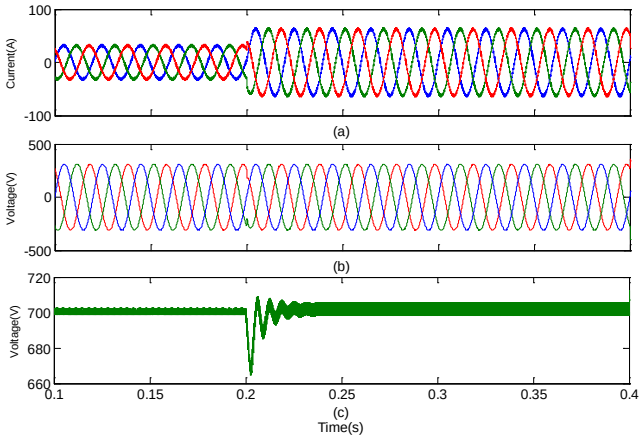

Fig. 10 Impedance converter control system function in the presence of ideal voltage source, (a) load current, (b) load voltage, (c) capacitor voltage C1

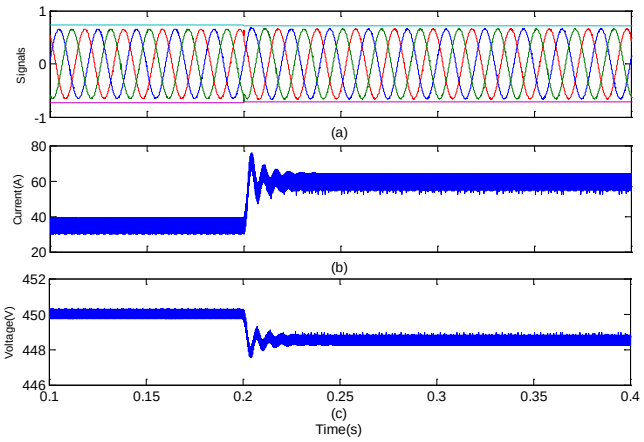

Fig. 11 System response with the ideal voltage source to load variations (a) Modulation signals, (b) DC source current, (c) Output voltage of DC source

As shown in Figures 10 and 11, the performance of the system with a perfect voltage source is quite desirable, and there is no evidence of instability and disturbance in the performance of the modulation system. This section examines the performance of a fuel cell with a resistance of 6ohm and a 660V non-load voltage. In this part of the super capacitor is not used and the fuel cell is parallel with the same capacitor Cs = 100uF.

In Figure 12 a, the capacitor voltage C1 is shown. As can be seen clearly, due to load shift, the control system is no longer able to maintain the C1 capacitor voltage, which brings complete instability to the system. From Figure 12a it can be concluded that the use of fuel cell with high tonnage resistance leads to unsustainable operation of the system and cannot be easily used from this source. Fig. 12b shows modulation signals which is interfered and faced the system's modulation function with complete failure. With the intersection of direct lines with sine signal signals, the active modulation vectors are eliminated and the production of an AC voltage waveform is not possible. The system voltage on the AC side is shown in Fig. 12c

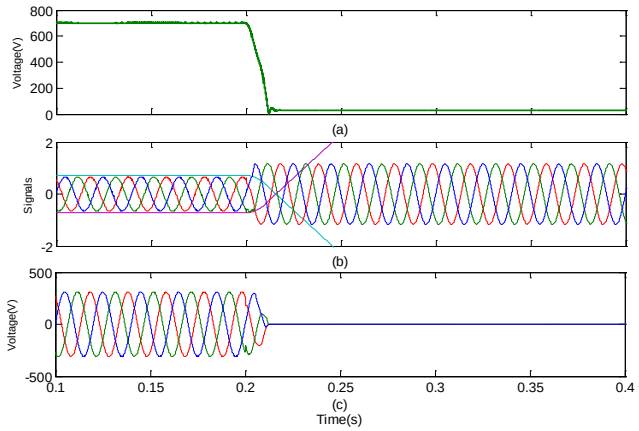

Fig. 12 The effect of using a fuel cell on the operation of the control system, (a) the capacitor voltage C1, (b) the modulation signals, (c) the voltage of network AC

In Figure 13 a, the fuel cell output voltage is displayed during doubling and unsustainability of the system. As can be seen, the fuel cell voltage drop is also very intense in this case, which increases the likelihood of network unsustainability. Figure 13b illustrates the flow of fuel cells.

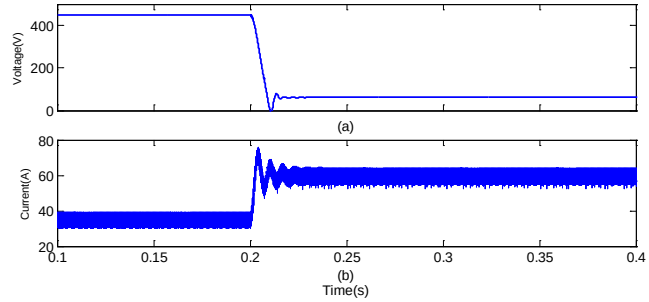

Fig. 13 System response to load changes in the use of fuel cell at the DC source side (a) Fuel cell voltage, (b) Fuel cell flow

After reviewing the function of the system with the source of the fuel cell on the DC side, we investigate the role of super capacitor in improving the system's performance. In this section, we Parallel a super capacitor Cs = 0.5F with simulated fuel cell in Figures 12 and 13. Regarding the bode diagrams depicted in Figures 7 to 9, it is predicted that the use of fuel cells will improve the performance of the system.

The charge current for a case that is used super capacitor in Figure 14a is shown. As shown in this figure, by doubling the load, the fuel cell inverter is able to double its production current. The load voltage is shown in Fig. 14b. As can be seen, using the super capacitor, the load voltage is stable and the waveform is not distorted. In Fig.

14c, the capacitor voltage C1 is shown. Contrary to Fig. 12, in which the capacitor voltage is unstable, in this case the control system continues to operate steadily. In this case, due to the use of super capacitor, the stability of the system is improved and the system is able to control the voltage of the C1 capacitor and the load voltage.

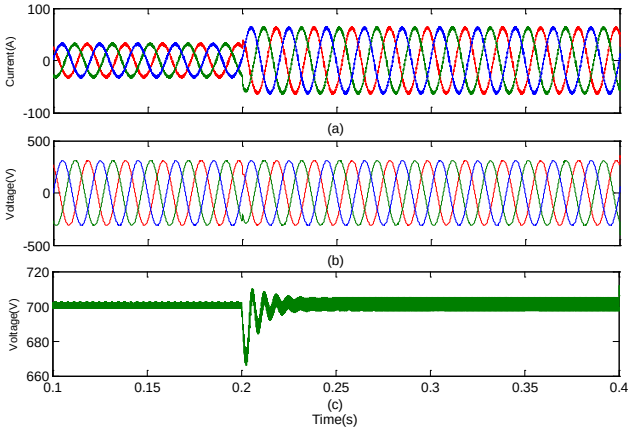

Fig. 14 Control system response to parallel fuel cell with supper capacitor, (a) AC current load, (b) load voltage, (c) capacitor voltage C1

In Fig. 15a, z-source inverter modulation signals are shown. As it is known, the signals are not interrupted and the z-source inverter modulation algorithm is correctly implemented. Figure 15b shows the flow of fuel cell and super capacitor collections. As can be seen, by increasing load, the amount of this flow increases. However, due to the presence of super capacitor, the fuel cell voltage changes are done as smooth as shown in Fig. 15c

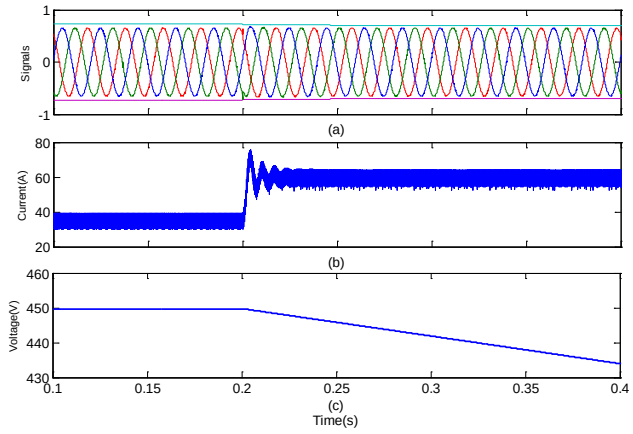

Fig. 15 Control system response to parallel fuel cell with supper capacitor, (a) modulation signals, (b) flow of supper capacitor and fuel cell, (c) fuel cell outlet voltage

From the simulations of Figs. 14 and 15, it can be concluded that the use of a super-capacitor in parallel with a fuel cell leads to the stability of the control system. In this case, as expected from bode diagrams 7-9, the system response is fast and the interference of the modulation signals does not occur. As shown in Fig. 9, using a super capacitor, the bode diagram of the fuel cell system and the quasi-z-source inverter is similar to a mode that in which the ideal voltage source is used. Similarly, the simulations of Figures 10 and 11 have a dynamic near to Figures 14 and 15, which confirms the bode diagram of Fig. 9. The simulations in Figures 14 and 15 shows that with the use of super capacitor, it can be achieved the optimal dynamic due to the use of the ideal voltage source.

5. Conclusion

In this paper, the dynamical modeling of the z-source inverter and fuel cell was used to design a suitable control system for a fuel cell system that feeding its local loads. It has been shown that the control systems designed for the z-source inverter are capable to provide optimal performance for an ideal voltage source on the DC side. However, the performance of the control system facing a true fuel cell with relatively large resistor faced with problem. In order to overcome this problem, a super capacitor was used in parallel with the fuel cell. Dynamic modeling shows that the use of supper capacitor led to the elimination of the effect of large fuel cell strength and increases the stability and dynamical speed of the control system. To simulate the modeling and compare the existence and absence of supper capacitor in the system, simulations performed in MATLAB / simulink software was used.

References

[1] Ghazanfari, M. Hamzeh, H. Mokhtari, and H. Karimi, “Active power management of multi hybrid fuel cell/supercapacitor power conversion system in a medium voltage microgrid,” IEEE Trans. Smart Grid., vol. 3, pp. 1903–1910, Dec 2012.

[2] T. S. Hwang, M. J. Tarca, and S. Y. Park, “Dynamic response analysis of dc-dc converter with supercapacitor for direct borohydride fuel cell power conditioning system,” IEEE Trans. Power Electron., vol. 27, pp. 3605–3615, Aug 2012.

[3] S. Samosir and A. H. M. Yatim, “Implementation of dynamic evolution control of bidirectional dc–dc converter for interfacing ultracapacitor energy storage to fuel-cell system,” IEEE Trans. Ind. Electron., vol. 57, no. 10, pp. 3468–3473, Oct. 2010.

[4] W. Liu, J. Chen, T. Liang, R. Lin, and C. Liu, “Analysis, design, and control of bidirectional cascaded configuration for a fuel cell hybrid power system,” IEEE Trans. Power Electron., vol. 25, no. 6, pp. 1565–1575, Jun. 2010.

[5] J.-C. Hwang, L.-H. Chen, and S.-N. Yeh, "A three-leg fuel-cell boost converter with novel digital-signal-processor based pulse-width odulation," in Proc. IEEE Region 10 Conf. (TENCON), Oct. 30–Nov. 2, 2007, pp. 1–4.
[6] M. H. Todorovic, L. Palma, and P. Enjeti, "Design of a wide input range dc–dc converter with a robust power control scheme suitable for fuel cell power conversion," in Proc. IEEE 19th Annu. Appl. Power Electron. Conf. Expo., 2004, vol. 1, pp. 374–379.
[7] F. Z. Peng, "Z-source inverter," IEEE Trans. Ind. Applicant., vol. 39, pp. 504–510, Mar/Apr 2003.
[8] Y. Huang, M. S. Shen, F. Z. Peng, and J. Wang, "Z-source inverter for residential photovoltaic systems," IEEE Trans. Power lectron., vol. 21, pp. 1776–1782, Nov 2006.
[9] S. Zhang, K. Tseng, D. M. Vilathgamuwa, T. D. Nguyen, and X. Wang, "Design of a robust grid interface system for PMSG-based wind turbine generators," IEEE Trans. Ind. Electron., vol. 58, no. 1, pp. 316–328, Jan. 2011.
[10] S. M. Dehghan, M. Mohamadian, and A.Y. Varjani, "A new variable-speed wind energy conversion system using permanent-magnet synchronous generator and z-Source inverter," IEEE Trans. Energy Convers., vol. 24, no. 3, pp. 714–724, Sep. 2009.
[11] Z. J. Zhou, X. Zhang, P. Xu, and W. X. Shen, "Single-phase uninterruptible power supply based on Z-source inverter," IEEE Trans. Ind. Electron., vol. 55, no. 8, pp. 2997–3003, Aug. 2008.
[12] J. Gajanayake, D. M. Vilathgamuwa, P. C. Loh, R. Teodorescu, and F. Blaabjerg, "Z-source-inverter-based flexible distributed generation system solution for grid power quality improvement," IEEE Trans. Energy Convers., vol. 24, no. 3, pp. 695–704, Sep. 2009.
[13] J. Jung and A. Keyhani, "Control of a fuel cell based z-source converter,"IEEE Trans. Ind. Electron., vol. 22, pp. 467–476, Jun 2007.
[14] M. Shen, A. Joseph, J. Wang, F. Z. Peng, and D. J. Adams, "Comparison of traditional inverters and z-source inverter for fuel cell vehicles," IEEE Trans. Power Electron., vol. 22, pp. 1453–1463, Jul 2007.
[15] F. Z. Peng, M. S. Shen, and K. Holland, "Application of z-source inverter for traction drive of fuel cell-battery hybrid electric vehicles," IEEE Trans. Power Electron., vol. 22, pp. 1054–1061, May 2007.
[16] F. Z. Peng, M. Shen, and Z. Qian, "Maximum boost control of the Z-source inverter," IEEE Trans. Power Electron., vol. 20, no. 4, pp. 833 838, Jul./Aug. 2005.
[17] M. Shen, J. Wang, A. Joseph, and F. Z. Peng, "Constant boost control of the Z-Source inverter to minimize current ripple and voltage Stress," IEEE Trans. Ind. Applicat., vol 42, no. 3, pp. 770-778, May/June 2006.
[18] M. Zhu, K.Yu, and F. L. Luo, "Switched inductor z-source inverter," IEEE Trans. Power Electron., vol. 25, pp. 2150–2158, Aug 2010.
[19] W. Qian, F. Z. Peng, and H. Cha, "Trans-z-source inverters," IEEE Trans.Power Electron., vol. 26, pp. 3453–3463, Dec 2011.
[20] J. Gajanayake, L. F. Lin, G. Hoay, S. P. Lam, and S. L. Kian, "Extended boost z-source inverters," IEEE Trans. Power Electron., vol. 25, pp. 2642–2652, Oct 2010.
[21] W. Mo, P. C. Loh, and F. Blaabjerg, "Asymmetrical -source inverters," IEEE Trans. Ind. Electron., vol. 61, pp. 637–647, Feb 2014.
[22] J. Gajanayake, D. M. Vilathgamuwa, and P. C. Loh, "Small-signal and signal-flow-graph modeling of switched Z-source impedance network," IEEE Trans. Power Electron., vol. 3, no. 3, pp. 111-116, Sep. 2005.
[23] P. C. Loh, D. M. Vilathgamuwa, C. J. Gajanayake, Y. R. Lim, and C. W. Teo, "Transient modeling and analysis of pulse-width modulated Z-source inverter," IEEE Trans. Power Electron., vol. 22, no. 2, pp. 498 -507, Mar. 2007.
[24] J. B. Liu, J. G. Hu, and L. Y. Xu, "Dynamic modeling and analysis of Z-source converter—Derivation of AC small signal model and designoriented analysis," IEEE Trans. Power Electron., vol. 22, no. 5, pp. 1786–1796, Sep. 2007.
[25] Y. Li, S. Jiang, J. G. Cintron-Rivera, and F. Z. Peng, "Modeling and control of quasi-Z-Source inverter for distributed generation applications," IEEE Trans. Ind. Electron., vol 60, no. 4, pp. 1532-1541, Apr. 2013.